



euronoise

# Diffraction modeling in acoustic radiance transfer method

S. Siltanen and T. Lokki

Helsinki University of Technology, P.O.Box 5400, 02015 TKK, Finland
samuel.siltanen@tml.hut.fi

The room acoustic radiance transfer method is a solution to recently presented room acoustics rendering equation which formulates the mathematical basis for all the ray-based (geometrical) room acoustic modeling algorithms. The basic acoustic transfer method gives as accurate results as the state-of-the-art commercial room acoustic modeling software. However, the basic method still lacks, e.g., diffraction modeling and modeling of complex reflections from surfaces. In this paper we extend the room acoustics rendering equation with diffraction kernel. In addition, we present one diffraction modeling method which can be used with the acoustic radiance transfer method. The method is a Biot-Tolstoy-based solution and it is shown to given accurate results in a case study.

# 1 Introduction

Geometric modeling of acoustics uses the laws of optics to trace the sound paths in the medium. Rays can be used to present wave fronts propagating perpendicular to them. This is a relatively safe assumption when the modeled wave length is much smaller than the dimensions of the bounding objects. However, at lower frequencies, the premise of the geometrical acoustics breaks.

The acoustic field can be described by a set of equations. In the most simple form, the wave equation for pressure $p$ might be written as

$$\frac{\partial^2 p}{\partial t^2} - c_0^2 \nabla^2 p = 0, \tag{1}$$

where $t$ is time and the constant $c_0$ depends on the medium. It is obvious that the pressure field must be continuous. However, this is not true in the "shadow"-boundaries in the geometric modeling approach. Thus, without diffraction modeling the results are inaccurate, in particular at low frequencies.

Siltanen et al. presented the room acoustics rendering equation which models energetic behavior of all the effects of geometrical acoustics [1]. Also, based on that model, an acoustic radiance transfer method, which is capable of modeling arbitrary reflections in complex environments, has been implemented. However, non-geometrical effects such as diffraction cannot be modeled. In this paper, our goal is to improve that model by attaching diffraction modeling to it.

# 2 Related Work

Many approaches to diffraction modeling have been presented. Some works concentrate in finding analytical solutions for certain cases while others aim at practical approximations which can be easily utilized.

The most relevant related work in diffraction modeling regarding this paper are the models based on the Biot-Tolstoy solution [2]. Biot and Tolstoy derived an accurate analytical solution for an infinite wedge or corner of a perfectly specularly reflecting material. Later, Medwin et al. interpreted their solution according to Huygens' principle as a total contribution from infinitely many point sources along the edge and used that view as a basis for deriving the corresponding solution for finite wedges or corners [3]. Svensson et al. presented this model in a form suitable for room acoustics modeling and discussed the practical details of the numerical evaluation of the integrals in the model [4]. The numerical stability of the evaluation in the case of singularities in the formulas was further improved by Svensson and Calamia [5].

Other approach to the diffraction modeling is Kirchhoff diffraction approximation [6], which, however, has been shown to be inaccurate in certain cases [7, 8]. The geometrical theory of diffraction [9] has also been used in acoustics, e.g., with the radiative transfer method [10].

# 3 Extending the room acoustics rendering equation

The room acoustics rendering equation [1] is based on the assumptions of geometric acoustics. The sound is assumed to behave like rays in optics. The acoustic attributes are defined on the surfaces of the model. The equation is

$$\begin{aligned} \ell(x', \Omega) &= \ell_0(x', \Omega) \\ &\quad + \int_{\mathcal{G}} R(x, x', \Omega) \ell(x, \Omega_{x \to x'}) \mathrm{d}x, \end{aligned} \tag{2}$$

where $\ell_0$ is the primary radiance from the surface, the integral is over the whole geometry $\mathcal{G}$, $\ell(x, \Omega_{x \to x'})$ is the radiance arriving at surface point $x'$ from another surface point $x$, and $R$ is the reflection kernel which takes into account the visibility between the two points, propagation delay, attenuation due to distance, and reflection from the material. Effects of medium absorption can be handled separatelly and taken into account in the detection.

Sound sources that cannot be modeled as surfaces (e.g. point sources) are taken into account by projecting their radiation on the surfaces, using the reflection model, i.e. acoustic BRDF, to compute the outgoing radiance, and conceptually taking the once-reflected radiance as primary radiation of the surface.

The final detection ($d$) is defined as a sum of the detection from the non-surface-like sources ($d_D$) and the detection from the surfaces ($d_\ell$):

$$d(t) = d_D(t) + d_\ell(t). \tag{3}$$

This presentation of the acoustic radiance captures all the effects that can be modeled by geometrical acoustics.

However, diffraction, by definition, cannot be modeled by using geometrical acoustics. Let us assume that diffraction occurs in connection to the singularities in geometry (points where the surface normal is not unambiguously defined) and that it can be modeled by some unknown method. The detection becomes:

$$d(t) = d_D(t) + d_\ell(t) + d_F(t), \tag{4}$$

i.e., the detected field is the sum of direct field, reflected field, and diffracted field ($d_F$). The rendering equation

needs also to be modified so that the singularities (denoted hereafter $\partial\mathcal{G}$) are included in $\mathcal{G}$ and if $x' \in \partial\mathcal{G}$ $R$ is replaced by the diffraction kernel $D_\omega$ which depends on the type of the singularity and the modeled frequency. That is:

$$\begin{aligned}\ell(x',\Omega) &= \ell_0(x',\Omega) \\ &\quad + \int_{\mathcal{G}} D_\omega(x,x',\Omega)\ell(x,\Omega_{x\to x'})\mathrm{d}x, \\ &\quad \text{when } x' \in \partial\mathcal{G}. \end{aligned} \tag{5}$$

The presented framework is very flexible since any reasonable diffraction model can be used as $D_\omega$.

Finally, let us define the detection functions:

$$\begin{aligned} d_D(t) &= \sum_{x_s} \Delta(\Omega_{x_s\to x_r}, \mathcal{HV}(x_s,x_r)\frac{S_r}{4\pi r^2}P_s(\Omega_{x_s\to x_r})) \\ d_\ell(t) &= \int_{\mathcal{G}\setminus\partial\mathcal{G}} \Delta(\Omega_{x\to x_r}, \mathcal{HV}(x,x_r) \\ &\quad \frac{S_r}{r^2}\ell(x,\Omega_{x\to x_r})max(\mathbf{n}_x\cdot\mathbf{u}_{x\to x_r},0)\mathrm{d}x \\ d_F(t) &= \int_{\partial\mathcal{G}} \Delta(\Omega_{x\to x_r}, \mathcal{HV}(x,x_r) \\ &\quad \frac{S_r}{r^2}\ell(x,\Omega_{x\to x_r})\mathrm{d}x, \end{aligned} \tag{6}$$

where $\mathcal{H}$ is an operator presenting medium absorption effects. $\mathcal{V}$ is a visibility function which equals one when the points given to it as attributes are visible to each other and zero otherwise. $P_s$ is the power of the source. $S_r$ is the delay operator for distance $r$ between the two points in each equation. $\mathbf{n}$ and $\mathbf{u}$ are normal and unit direction vectors, respectively. Finally, $\Delta$ is a function which maps the incoming radiance to observed sound pressure.

# 4 Applying Biot-Tolstoy-Medwin model

Since the original acoustic rendering equation already describes an energy balance, adding a new term to the equation could potentially shake that balance and lead to an unphysical model. Handling the singularities as special cases allows the emitted energy to blead into shadow-zones. For the singularities having only an infitesimal area, they cover a zero solid angle of the angular space, seen from any point, and receive zero energy.

The diffraction term should be seen as a correction term to the geometrical acoustics solution. Thus, it can be negative in some cases. This is necessary for conserving the energy.

## 4.1 Separating reflection and visibility discontinuity components of the diffraction model

The original Biot-Tolstoy model is an exact solution for diffraction of a point source from an infinite wedge [2]. Later, Medwin et al. interpreted the given solution as a summation of secondary sources along the edge [3]. This interpretation allows derivations of the solution for finite edges. Svensson et al. derive such a model as a line-integral [4]. They give an expression for pressure $p$:

$$\begin{aligned} p_{\mathrm{diffr}}(t) = -\frac{\nu}{4\pi}\int_{z_1}^{z_2} q\left[t-\frac{m(z)+l(z)}{c}\right] \\ \times\frac{\beta[\alpha(z),\gamma(z),\theta_S,\theta_R]}{m(z)l(z)}\mathrm{d}z, \end{aligned} \tag{7}$$

where $t$ is time (the impulse is emitted when $t=0$), $\nu$ equals $\pi/\theta_w$ ($\theta_w$ is the opening angle of the wedge), $z_1$ and $z_2$ are the end points of the edge in a coordinate system where z-axis is along the edge, $q$ is the emitted signal, $c$ is the speed of sound, and angles $\theta_S$ and $\theta_R$ are directions of the sources and receiver, respectively, around the z-axis. Variable $m(z)$ is the length of the paths of diffraction from the source to the edge point $z$ and variable $l(z)$ is the length of the rest of the path to the receiver. Angles $\alpha(z)$ and $\gamma(z)$ are the angles between these paths and a line perpendicular to z-axis on a plane defined by the path and the edge. Let us set $z=0$ for the source and $z=z_R$ for the receiver, and let $r_S$ and $r_R$ be the direct distances from the z-axis to the source and receiver, respectively. Then, using basic trigonometry, we get

$$m(z) = \sqrt{r_S^2+z^2} \tag{8}$$

$$l(z) = \sqrt{r_R^2+(z-z_R)^2} \tag{9}$$

$$\alpha(z) = \tan^{-1}\frac{z}{r_S} \tag{10}$$

$$\gamma(z) = \tan^{-1}\frac{z}{r_R}. \tag{11}$$

For infinitely hard surfaces $\beta$-function is defined as

$$\begin{aligned}\beta_{\mathrm{hard}}(\alpha,\gamma) &= \beta_{++}(\alpha,\gamma)+\beta_{+-}(\alpha,\gamma)+ \\ &\quad \beta_{-+}(\alpha,\gamma)+\beta_{--}(\alpha,\gamma)\end{aligned} \tag{12}$$

$$\beta_{\pm\pm}(\alpha,\gamma) = \frac{\sin[\nu(\pi\pm\theta_S\pm\theta_R)]}{\cosh[\nu\eta(\alpha,\gamma)]-\cos[\nu(\pi\pm\theta_S\pm\theta_R)]} \tag{13}$$

$$\eta(\alpha,\gamma) = \cosh^{-1}\frac{1+\sin\alpha\sin\gamma}{\cos\alpha\cos\gamma}. \tag{14}$$

Then the boundary condition is:

$$\mathbf{u}\cdot\mathbf{n}=0, \tag{15}$$

where $\mathbf{u}$ is the total particle velocity at the surface and $\mathbf{n}$ is the surface normal. In effect, the incoming wave is totally reflected on the surface and its phase (considering particle velocity) is shifted by 180 degrees.

On the other hand, the $\beta$-function can be defined for soft or pressure-release surfaces and the expression given by Kinney et al. [11] is

$$\begin{aligned}\beta_{\mathrm{soft}}(\alpha,\gamma) &= -\beta_{++}(\alpha,\gamma)+\beta_{+-}(\alpha,\gamma)+ \\ &\quad \beta_{-+}(\alpha,\gamma)-\beta_{--}(\alpha,\gamma),\end{aligned} \tag{16}$$

where the boundary condition is simply

$$p=0, \tag{17}$$

where $p$ is the pressure at the surface. Again, the wave is totally reflected on the surface, but its phase is not shifted.

Now the diffraction pressure can be separated to the diffraction caused by the reflection and to the diffraction caused by visibility discontinuities. Let there be two wedges or corners with exactly the same geometry, but different materials. The first one is of infinitely hard material and the second one has the pressure-release property. The acoustic fields for the pressure can be described in both cases as:

$$p_{\text{total,hard/soft}} = p_{\text{dir}} + p_{\text{refl,hard/soft}} + p_{\text{diffr,disc}} + p_{\text{diffr,hard/soft,refl}}, \tag{18}$$

where the pressure terms are for the total field, direct field, reflected field, and diffracted field for discontinuities and reflection, respectively. The sum of the diffraction components equals the result of the (modified) Biot-Tolstoy model, presented above:

$$p_{\text{diffr,hard/soft}} = p_{\text{diffr,disc}} + p_{\text{diffr,hard/soft,refl}} \tag{19}$$

Now, let us add the fields together:

$$p_{\text{total,hard}} + p_{\text{total,soft}} = 2p_{\text{dir}} + 2p_{\text{diffr,disc}}, \tag{20}$$

where the reflection terms have disappeared since they were otherwise equal, but there was a 180-degree phase shift, so the reflected wave fields annulled each other. Then, we have one of the diffraction components separated:

$$\begin{aligned} p_{\text{diffr,disc}} &= \frac{1}{2}\left(p_{\text{total,hard}} + p_{\text{total,soft}}\right) - p_{\text{dir}} \\ &= \frac{1}{2}\left(p_{\text{diffr,hard}} + p_{\text{diffr,soft}}\right). \end{aligned} \tag{21}$$

Since integration is a linear operator and the integrand is linear in relation to the $\beta$-functions, we can write a same kind of relation also for them:

$$\begin{aligned} \beta_{\text{disc}} &= \frac{1}{2}\left(\beta_{\text{hard}} + \beta_{\text{soft}}\right) \\ &= \frac{1}{2}\left(\beta_{++}(\alpha,\gamma) + \beta_{+-}(\alpha,\gamma)\right. \\ &\quad +\beta_{-+}(\alpha,\gamma) + \beta_{--}(\alpha,\gamma) \\ &\quad -\beta_{++}(\alpha,\gamma) + \beta_{+-}(\alpha,\gamma) + \\ &\quad \left.\beta_{-+}(\alpha,\gamma) - \beta_{--}(\alpha,\gamma)\right) \\ &= \beta_{+-}(\alpha,\gamma) + \beta_{-+}(\alpha,\gamma). \end{aligned} \tag{22}$$

Inserting this $\beta_{\text{disc}}$ into the expressions for the pressure, the result is a diffracted field without the reflection component (for hard surface)

$$\beta_{\text{refl}} = \beta_{++}(\alpha,\gamma) + \beta_{--}(\alpha,\gamma). \tag{23}$$

This separation allows us to formulate the reflected diffraction for surfaces with arbitrary specular reflection coefficients by weighting the $\beta_{\text{refl}}$ coefficient accordingly. The weighting factor can be set to zero if there are no specular reflections or other kinds of diffraction components can be used for other kinds of reflections which cause discontinuities to the acoustic field, while the $\beta_{\text{disc}}$ component remains the same.

## 4.2 Continuity on zone boundaries

There would be four zones in the diffracted field. Figure 1 shows these zones in relation to the source and the wedge. Usually only three zones are given, but since the reflection model can contain also non-specular components a new zone must be introduced. If only specular reflections are used, Zones II and III are merged to one zone.

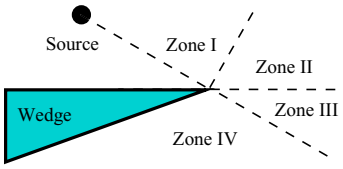


Figure 1: Zones in the diffracted field in relation to the source and the wedge.

The response in Zone I consists of the direct field, specularly and non-specularly reflected fields, and diffracted field. From Zone II onwards the specularly reflected field does not contribute to the response. From Zone III onwards also the non-specular part of the reflected field seizes to affect the result. And, in Zone IV, the direct field disappears, thus leaving only the diffracted field.

The diffraction components assure continuity of the field on two of the boundaries: I-II and III-IV. Since the diffracted field is continuous over II-III boundary, the only discontinuity might come from the fact that the non-specular component suddenly becomes zero when moving from Zone II to Zone III. However, the non-specular part of the BRDF is weighted by the cosine of the angle between the surface normal and the outgoing direction. Thus, it can be shown that if the angular dependency of the non-specular reflection model has zero derivative on the zone boundary, the wave equation holds and there is no discontinuity between zones II and III. This is true in the case of ideal diffuse reflection. If the derivate would be non-zero on the boundary, a diffraction component corresponding to that reflection model should be added to the solution.

## 4.3 Singularities at boundaries

The $\beta$-function has singularities when the denominator of at least one of the $\beta_{\pm\pm}$-functions equals zero. This can happen only when both $\cosh[\nu\eta(\alpha,\gamma)]$ and $\cos[\nu(\pi \pm \theta_S \pm \theta_R)]$ equal one, since $\cosh x \geq 1$ and $\cos x \leq 1$ with any real-valued $x$. A closer examination of the cosine term shows that this is possible only on the boundaries of the shadow (Zone IV) and specular regions (Zone I). Even then, $\alpha$ and $\gamma$ must equal zero. The singularities can easily be handled as special cases when evaluating the integrals [5].

## 4.4 Energetic approach and pressures

Since Biot-Tolstoy-Medvin diffraction model is given for pressures, it cannot be directly applied to the rendering equation which uses an energetic model. In an ideal case, intensity of the diffracted field can be computed as

$$I_{\text{diffr}} = \frac{|p_{\text{diffr}}|^2}{\rho c}. \tag{24}$$

The intensity is thus proportional to the square of pressure. Also the differential quantities, such as radiance and irradiance, have the same kind of dependency on

pressure. However, the expression always produces positive values. Thus, if the intensity produced by the the geometrical acoustics is directly added up with the diffracted intensity, the result is that more energy is brought to the system which is physically incorrect.

By examining the behaviour of the diffracted field, it can be seen that near the specular boundary the pressure response has a negative amplitude in Zone I and positive amplitude in Zone II so that they are equal on the boundary if the absolute value of the amplitude is half the amplitude of the specular field. Correspondingly, there are negative and positive amplitudes with the half of the absolute value of the amplitude of the direct field in Zones III and IV near the shadow boundrary. Signs can be assigned to the energies so that near the boundary the sign is negative in Zones I and III, and positive in Zones II and IV. By integrating over the whole open angle, it can be shown that the total diffracted energy sums up to zero, thus preserving the energy.

# 5 Results

The modified Biot-Tolstoy model explained in the previous section was implemented to the acoustic radiance transfer method. To model the diffraction by an edge, it has to be split into short segments. The incoming radiance is computed for each segment separately and the diffracted radiance is computed by the Biot-Tolstoy model. The diffracted radiance is stored into the segments as "diffraction BRDFs", presenting the contribution by the source to all the outgoing directions. This corresponds to the "initial shoot" phase in the acoustic radiance transfer method [1]. Then, when computing the diffracted response received at a certain point, the contributions of the segments to that direction can be read directly from the BRDF. The total response is a sum of all visible segments to the receiver. This corresponds to the "final gathering" phase in the acoustics radiance transfer method. When evaluating the integral in the Biot-Tolstoy model, the value of the integrand is computed using the values of the integrand at the end points of a segment and the trapezoid rule. In the time domain, the contribution is usually spread over several samples in the response and the energy is equally divided among them.

Results were computed in the case of a simple hard wedge with a 270 degree opening angle, see Fig. 2. The edge is situated along the z-axis and extends from -10 meters to +10 meters. The other half-plane limiting the solid part of the wedge is along the xz-plane ($x > 0$), and the other plane is that plane rotated by 270 degrees around the z-axis. The source is placed at distance of 1 meter from the edge and rotated 30 degrees from the first plane around the z-axis, and 1.5 meters from the origin in the z-direction. The receivers are placed at a distance of 2 meters from the edge with varying rotation angles around the z-axis, with the same z-coordinate as the source.

The comparison is done to the results produced by the model of Svensson et al. [4]. The analytical results are computed for each sample in the response, which is 100 ms long with a sampling frequency of 44100 Hz. In the case of the first sample, the approximations by Svensson and Calamia [5] are used to avoid numerical instability due to singularities in the Biot-Tolstoy formulas.

## 5.1 Discussion

Figure 2 shows that the diffraction model implemented to the acoustic radiance tranfer method produces quite similar results to the Svensson et al. model as expected, since they both use the Biot-Tolstoy model. The first spike seen in figures with a receiver angle of 30-210 degrees is the direct sound. The second spike in figures with a receiver angle of 30-150 degrees is the specular reflection. The diffraction tail forms the rest of the responses. There is an obvious step in the otherwise smooth response at approximately 2200 samples, the effect of the shorter half of the edge disappearing. The diffraction tail ends a little before 3000 samples, where the effect of the other half of the edge seizes too.

The segmentation of the edge causes little steps to the response. Increasing the number of segments improves the results and when the segment length is so short that each segment contributes to only one sample, the steps disappear. To improve the results without increasing the number of segments can be done by computing the sample range which is affected by each segment and using the analytical model for each sample in that range. This approach would be more time consuming and it does not improve the directional accuracy of the model, which is dependent on the discretization of the edge. Finding ways to improve the accuracy of the diffracted response is still a topic of future research. The techniques introduced by Calamia and Svensson could be utilized [12].

The results show that the model works with a single edge. Since the diffraction model is formulated so that it fits to the acoustics radiance transfer method [1], arbitrarily complicated models, within the limits of computational resources, can be modeled without changes in the presented model. Since the contributions are stored in the BRDFs attached to edge segments, the computation can be broken apart into iterative steps. Future research may show how to attach these steps to the iterative propagation in the acoustic radiance transfer method so that the computation converges.

# 6 Conclusion

The room acoustics rendering equation, representing all the effects of the geometrical acoustics, is generalized so that also diffraction can be taken into account. This is done by adding a general correction term to the equations. The choice of the diffraction model is free, but in this paper a Biot-Tolstoy-based solution is given. The results produced by this model in a case of a simple wedge are compared to those produced by the model of Svensson et al. [4]. In general, the agreement between the results is good, with minor exceptions caused by discretization error in the acoustic radiance transfer method. The method can be used in the case of more complicated models also.

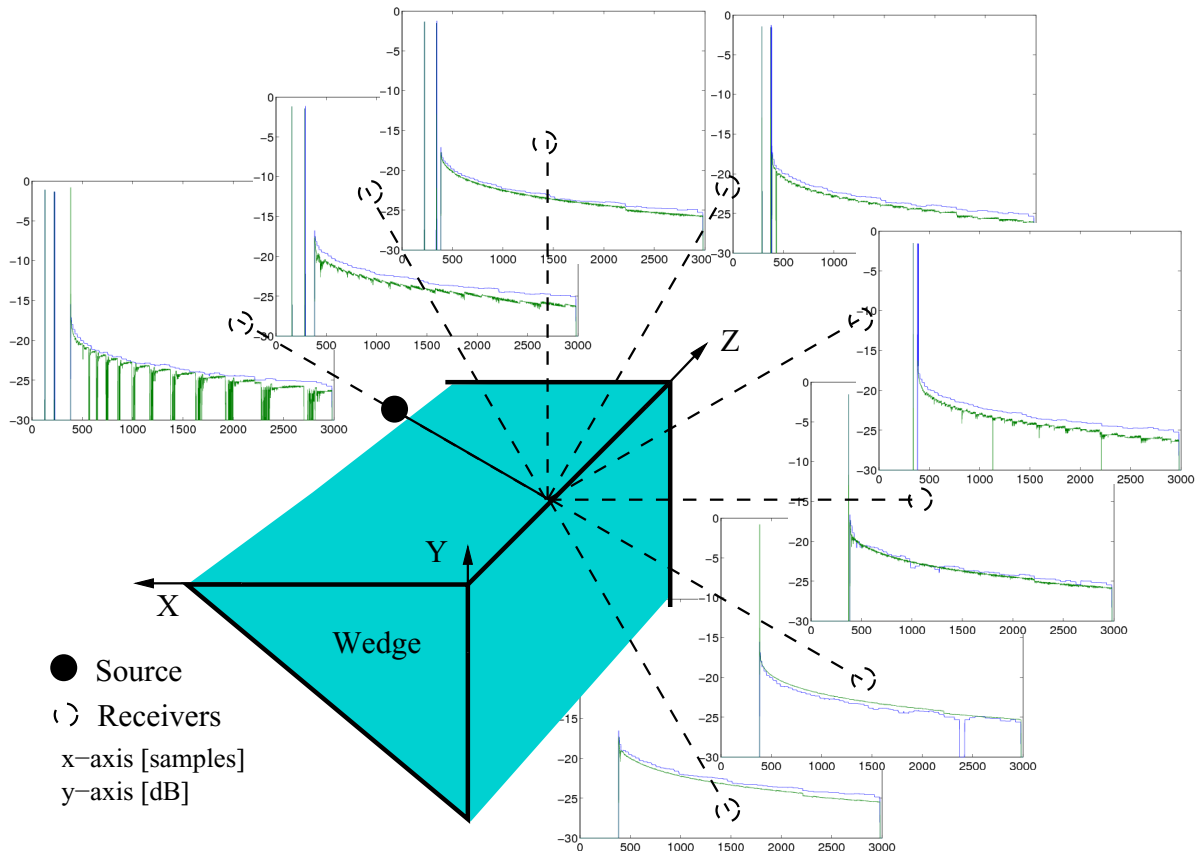


Figure 2: The results evaluated at several receiver points. The blue curve is prodoced by the acoustic radiance transfer method and the green curve by the Svensson et al. model. The figures for the receiver angles from 30 degrees to 240 degrees with a 30-degree step.

## Acknowledgments

This work has been supported by the Academy of Finland (project no. 119092).

## References

[1] S. Siltanen, T. Lokki, S. Kiminki, and L. Savioja. The room acoustics rendering equation. *J. Acoust. Soc. Am.*, 122(3):1624–1635, 2007.

[2] M. A. Biot and I. Tolstoy. Formulation of wave propagation in infinite media by normal coordinates with an application to diffraction. *J. Acoust. Soc. Am.*, 29(3):381–391, 1957.

[3] H. Medwin, E. Childs, and G.M. Jebsen. Impulse studies of double diffraction: A discrete huygens interpretation. *J. Acoust. Soc. Am.*, 72(3):1005–1013, 1982.

[4] U.P. Svensson, R.I. Fred, and J. Vanderkooy. An analytic secondary source model of edge diffraction impulse responses. *J. Acoust. Soc. Am.*, 106(5):2331–2344, 1999.

[5] U.P. Svensson and P.T. Calamia. Edge-diffraction impulse responses near specular-zone and shadow-zone boundaries. *Acta Acustica united with Acustica*, 92(4):501–512, 2006.

[6] A.W. Trorey. Diffractions for arbitrary source-receiver locations. *Geophysics*, 42(6):1177–1182, 1977.

[7] G.M. Jebsen and H. Medwin. On the failure of the kirchhoff assumption in backscatter. *J. Acoust. Soc. Am.*, 72(5):1607–1611, 1982.

[8] G.V. Norton, J.C. Novarini, and R.S. Keiffer. An evaluation of the kirchhoff approximation in predicting the axial impulse response of hard disk. *J. Acoust. Soc. Am.*, 93(6):3049–3056, 1993.

[9] R.G. Kouyoumjian and P.H. Pathak. A uniform geometrical theory of diffraction for an edge in a perfectly conducting surface. *Proceedings of the IEEE*, 62(11):1448–1461, 1974.

[10] E. Reboul, A. Le Bot, and J. Perret-Liaudet. Radiative transfer equation for multiple diffraction. *J. Acoust. Soc. Am.*, 118(3):1326–1334, 2005.

[11] W.A. Kinney, C.S. Clay, and G.A. Sandness. Scattering from a corrugated surface: Comparison between experiment, helmholtz-kirchhoff theory, and the facet-ensemble method. *J. Acoust. Soc. Am.*, 73(1):183–194, 1983.

[12] P.T. Calamia and U.P. Svensson. Edge subdivision for fast diffraction calculations. In *Proceedings of 2005 IEEE Workshop on Applications of Signal Processing to Audio and Acoustics*, pages 187–190, New Paltz, NY, 2005.